Ziprasidone Suppresses Pancreatic Adenocarcinoma Cells Proliferation by Targeting GOT1 to Trigger Glutamine Metabolism Reprogramming

Yueying Yang
Shenyang Pharmaceutical University
Fei Han
Shenyang Pharmaceutical University
Mingxue Li
Shenyang Pharmaceutical University
Mengzhu Zheng
Huazhong University of Science and Technology
Xiaoxia Gu
Huazhong University of Science and Technology
Hua Li
Shenyang Pharmaceutical University
Lixia Chen (syzyclx@163.com)
Shenyang Pharmaceutical University https://orcid.org/0000-0003-2196-1428

Research Article

Keywords: ziprasidone, GOT1 inhibitor, glutamine metabolism, metabolomics analysis, pancreatic cancer

Posted Date: July 16th, 2021

DOI: https://doi.org/10.21203/rs.3.rs-604303/v1

Version of Record: A version of this preprint was published at Journal of Molecular Medicine on February 25th, 2022. See the published version at https://doi.org/10.1007/s00109-022-02181-8.

Abstract

Pancreatic ductal adenocarcinoma (PDAC) is a fatal malignant tumor that no effective treatment has been found. The redox state and proliferative activity of PDAC cells are maintained by the conversion of aspartic acid in the cytoplasm into oxaloacetate though aspartate aminotransferase 1 (GOT1). Therefore, GOT1 inhibitors as a potential approach for treating PDAC have attracted more attention of researchers. Ziprasidone effectively inhibited GOT1 in a non-competitive manner. The potential cytotoxicity and anti-proliferation effects of ziprasidone against PDAC cells *in vitro* and *in vivo* were evaluated. Ziprasidone can induce glutamine metabolism disorder and redox state imbalance of PDAC cells by targeting GOT1, thereby inhibiting proliferation, preventing migration and inducing apoptosis. Ziprasidone displayed significant *in vivo* antitumor efficacy in SW1990 cell-derived xenografts. What's more, knockdown of GOT1 in SW1990 reduced the anti-proliferative effects of ziprasidone. As a novel GOT1 inhibitor, ziprasidone may be a lead compound for the treatment of PDAC.

Highlights

1. Small molecule inhibitors targeting GOT1 may provide an therapeutic target in PDAC.

2. Ziprasidone effectively inhibited GOT1 enzyme in a non-competitive manner.

3. Ziprasidone repressed glutamine metabolism and inhibited the growth of tumor *in vivo*.

4. Knockdown of GOT1 decreased the anti-proliferative effects of ziprasidone.

1. Introduction

Pancreatic ductal carcinoma (PDAC), a deadly type of cancer, is listed as the second leading cause of cancer-related deaths in the United States by 2020 [1,2]. Because of the lack of early detection of biomarkers, the lethality of PDAC is largely due to the late onset of symptoms when the cancer has reached metastasis. The 5-year survival rate of pancreatic cancer is only 8% [3], prompting researchers to identify new targets for PDAC therapy.

Metabolic reprogramming is a distinctive feature of tumor cells. The entry of glutamine metabolites into the anabolic pathway is one of the distinctive features of tumor cells [4]. Emerging studies indicate that the KRAS-regulated non-classical glutamine (Gln) metabolic pathway could promote the proliferation and growth in partial PDAC cells [5]. As a nutrient for tumor cells, Gln provides a carbon source for the TCA cycle, a nitrogen source for nucleotide biosynthesis and hexosamine [6,7]. The formation of glutamine-derived aspartate was promoted by the up-regulation of GOT1 in PDAC. GOT1 converted aspartate into oxaloacetate in the cytoplasm. Subsequently, this oxaloacetate is converted into malate and then pyruvate, which ultimately increasing the $NADPH/NADP^+$ ratio to maintain ROS balance [5]. Studies have shown that the proliferation of PDAC cells was inhibited by reducing the GOT1 expression without

affecting the growth of normal tissue cells [6]. GOT1-targeted inhibitors have been reported to provide a much-needed treatment for pancreatic ductal carcinoma [8].

To date, few selective small molecule inhibitors of GOT1 have been reported. Among them, aminooxyacetate (AOA) decreased the flux of ^{13}C-glucose-derived carbons into glutamate and uridine by targeting GOT1 in MDA-MB-231 cells [9]. 4-(1H-indol-4-yl)-N-phenylpiperazine-1-carboxamide was found to be a potential inhibitor of GOT1 though a high-throughput screening with 800,000 compounds [10]. The GOT1 inhibitor iGOT1-01 discovered by high-throughput screening exhibits potential metabolic and growth inhibitory activities, but the specific binding site and mechanism are not clear. [11].

Due to the important role of GOT1 in maintaining the PDAC cells redox homeostasis, the discovery of potential inhibitors of GOT1 may be a new strategy for the treatment of PDAC. We have long been committed to discovering GOT1 inhibitors with good anti-PDAC activity and exploring the mechanism in depth. Aspulvinone O, a natural GOT1 inhibitor, has been found to trigger glutamine metabolism and suppress PDAC cells proliferation in our previous study [12].

Drug repurposing, also referred to as drug repositioning or reprofiling, is aiming at discovering new indications of existing drugs. Taking into account the malignancy of PDAC and the urgency of treatment, we tried to discover promising existing drugs for the treatment of PDAC through drug repurposing. Ziprasidone, a selective monoamine antagonist, has strong binding affinity with dopamine (D2/3), serotonin (5-HT2A, 5-HT2C, 5-HT1A, 5-HT1D) and α1-adrenergic receptors, which is used for the treatment of acute agitated symptoms in patients with schizophrenia [13]. Ziprasidone induces glutamine metabolism disorders in SW1990 cells by inhibiting the catalytic activity of GOT1, which significantly suppresses the proliferation of SW1990 cell-derived xenografts. Briefly, the discovery of the new application of ziprasidone provides a novel strategy for PDAC treatment.

2. Materials And Methods

2.1 Reagents

Ziprasidone (Code: MB1289, China) was purchased from MCE (Cat # HY-14542). Antibodies of GOT1, caspase 9, caspase 3, Phospho-JNK-1/2, Phospho-p38, LC3-ii, β-actin, PARP, Cleaved PARP, AKT, PTEN, Erk-1, p-Erk, Bcl-2, Bax, and Bcl-X_L were obtained from ABclonal.

Other reagents were as follows: EdU (Guangzhou RiboBio Co., Ltd.), DAPI (Molecular Probes). Cell lines, HepG2 (HB-8065), HCT116 (CCL-247), HCC1806 (CRL-2335), L929 (CRL-6364), PANC-1 (CRL-1469), SW620 (CCL-227), AspC-1 (CRL-1682), SW480 (CCL-228), SW1990 (CRL-2172), A549 (CCL-185), HT1080 (CCL-121) were purchased from ATCC.

2.2 GOT1 protein expression and purification

Briefly, GOT1 protein was expressed by cloning human GOT1 ORF (GeneBank: NC_000010.11) into a pET28a vector containing 6 His-tag. The recombinant plasmids were transduced into *E. coli* strain BL21 and cultured in Luria-Bertani medium at 37 °C, and then 0.4 mM IPTG was added at 18 °C to induce GOT1 protein expression for 18 h. The details of GOT1 protein purification were as previously reported [14, 15]. The purified GOT1 protein is quick-frozen and stored at -80°C for subsequent experiments.

2.3 GOT1 inhibition assay

An enzyme activity reaction system was constructed *in vitro* to evaluate the inhibitory activity of ziprasidone on recombinant GOT1 protein by monitoring the change in absorbance at 340 nm caused by the reduce of NADH on Microplate Reader (BioTek, USA). Total 100 μL reaction system, contained 0.1 mg/mL GOT1, 1 mM α-KG, 4 mM aspartic acid, 1 mM NADH and 1 unit/mL malate dehydrogenase [15].

2.4 Microscale Thermophoresis (MST) assay

The binding affinity between ziprasidone and GOT1 were determined by MST according to the instruction of Monolith™ NT.115 Protein Labeling Kit RED-NHS (Cat # MO-L011). GOT1 was dispersed into 20 mM HEPES (pH 7.5) solution with final concentration of 10 μM and labelled by the RED-NHS dye. Ziprasidone was diluted to different concentrations based on gradient dilution and was incubated with the labeled GOT1 for 20 min. All samples were tested on the Monolith NT.115 instrument for their binding affinity to GOT1 (Nano Temper Technologies, Germany) [15].

2.5 Molecular Docking

The crystal structure of GOT1 (PDB ID: 3II0) was downloaded from the Protein Data Bank (http://www.rcsb.org/). The docking was executed through ICM 3.8.2 modeling software (MolSoft LLC, San Diego, CA). The ligand binding sites was selected though ICM software graphical tools for the molecular docking. The potential energy diagram of the receptor was calculated with default parameters. According to the Monte Carlo procedure 30, the numerous conformations of ligands were tested. Finally, the most promising conformations of the ligand were selected with the lowest-energy [16].

2.6 Cell viability

The MTT assay was used to evaluate the cell viability after compound treatment. 5×10^3 cells/well were seeded in 96-well plates until it converges to 80%, and then administrated with different concentrations of ziprasidone (0-100 μM). 100 μL of 5 mg/mL MTT was added after ziprasidone treatment for 24 h. After incubated for 4 h at 37^{o}C, DMSO (100 μL/well) was added to dissolve the formazan crystals. The absorbance was measured at 490 nm with a microplate reader.

2.7 Apoptosis analysis

After treating SW1990 cells with 20 μM and 40 μM ziprasidone for 24 h, the cells were collected and incubated with Annexin V-FITC/PI for staining. The specific operation details referred to the Roche Annexin-V-FLUOS Staining Kit (Cat # 11858777001). Fluorescence was determined by FACS Verse flow cytometer.

2.8 Colony formation assay

SW1990 cells were inoculated in a 6-well plate at 200/well and cultured for 24 h. Then, SW1990 cells were treated with different concentrations of ziprasidone. During the culture, the fresh medium containing ziprasidone was changed every three days until visible colonies were formed. SW1990 colonies were stained with 1% crystal violet, then washing with PBS for three times and counting colonies containing more than 50 cells.

2.9 Immunofluorescence staining

Briefly, cells were seeded into 96-well plates for 12 h and were treated with different concentrations of ziprasidone for 24 h, 4% paraformaldehyde for 20 min, 0.2% Triton X-100 for 10 min, and incubated with 50 μM EdU for 2 h. The EdU proliferation experiment was performed according to the kit instruction of the previous description [17].

For the Hoechst 33342 staining, SW1990 cells were seeded into 96-well plates with 1×10^4/well and cultured for 12 h, then replaced with fresh DMEM containing DMSO or 10-40 μM ziprasidone, cultured for another 12 h, and dyed with 100 μL 20 μM Hoechst 33342 for 10 min. The morphology of nuclear chromosomes was observed under a fluorescence microscope at 340 nm. (Nikon, Japan).

2.10 Transwell migration

First, 600 μL complete medium with ziprasidone were supplemented into the lower chamber, and then 5×10^4 SW1990 cells were dispersed in 100 μL DMEM medium without FBS in upper chamber. The cell colonies at the bottom of the membrane were stained with crystal violet and then observed and counted under a microscope (Nikon, Japan).

2.11 Wound scratch assay

SW1990 cells were cultured until the cell density reached about 85%, three straight scratches were made by 10 μL micro pipette tip per well. Wash the 6-well plates with PBS before treating the cells with different

concentrations of ziprasidone. At 0 h and 24 h after ziprasidone treatment, microscopic pictures were taken to analyze the compound's ability to inhibit cell migration.

2.12 Western blot assays

SW1990 cells were seeded into a 6-well plate at 5×10^5/well and cultured until the cell confluence was above 85%. SW1990 cells were treated with ziprasidone for 24 h and then collected. Cells were resuspended with RIPA lysis buffer (Beyotime Biotechnology) containing 0.1% PMSF to release total protein. The concentration of total protein was determined by BCA Protein Assay Kit (Beyotime Biotechnology). Total protein was separated by SDS-PAGE and transferred to PVDF membrane (Merck Millipore, 0.2 μm). The PVDF membrane was incubated with the primary antibody overnight at 4°C, and then with the secondary antibody for 2 h at room temperature, finally performed chemiluminescence imaging (Tanon 5200).

2.13 siRNA knockdown of GOT1

SW1990 cells were seeded into a 6-well plate at 5×10^5/well and cultured until the cell confluence was 90%-95%. Mix 100 pM siRNA with 5 uL Hieff Trans™ Liposomal Transfection Reagent and incubate for 20 min at room temperature. siRNA-liposome complexes treated SW1990 cells for 6 h and then replaced them with fresh DMEM medium and continued to culture for 48 h.

siRNA-1 Forward: 5'to3' CAG GUA AUG UGA AGA CAA UTT

siRNA-1 Reverse: 5'to3' AUU GUC UUC ACA UUA CCU GTT

siRNA-2 Forward: 5'to3' GCG CGU UGG UAC AAU GGA ATT

siRNA-2 Reverse: 5'to3' UUC CAU UGU ACC AAC GCG CTT

siRNA-3 Forward: 5'to3' AGA AAG UGG AGC AGA AGA UTT

siRNA-3 Reverse: 5'to3' AUC UUC UGC UCC ACU UUC UTT

2.14 Cellular thermal shift assay (CETSA)

CETSA (cellular thermal shift assay) is usually used to evaluate the targeting effect between the compound and the protein based on the principle that the ligand can improve the thermal stability of the target protein. SW1990 cells were cultured to more than 80% confluence, replaced with fresh DMEM containing DMSO or 30 μM ziprasidone, and cultured for another 12 h. SW1990 cells were heat-treated from 42°C to 52°C for 3 min. Specific experimental details referred to the previous description [18-20].

2.15 Measurement of ECAR and OCR

SW1990 cells were seeded in 24-well plates at a density of 5×10^4 and cultured for 12 h, and then treated with fresh DMEM medium containing 20 μM ziprasidone for 3 h. XF24 Extracellular Flux Analyzer (SeaHorse Bioscience) was used to determine the changes in oxygen consumption rate (OCR) and extracellular acidification rate (ECAR) of SW1990 cells after administration of ziprasidone. Experimental details were as previously reported [12].

2.16 Metabonomics experimental methods

The SW1990 cells were confluent to more than 80% and treated with 20 μM ziprasidone, and the control group was added with an equal volume of DMSO. After culturing for 24 h, we collected the cells and added 70% methanol aqueous solution to lyse on ice. The cells were lysed by repeated freezing and thawing of liquid nitrogen and the metabolites were dissolved in methanol aqueous solution. The supernatant is centrifuged to perform LC-MS/MS analysis. Parameter settings and operating mode for LC-ESI-MS/MS analysis were as previously described [17].

2.17 In vivo tumor xenograft study

CB-17/SCID mice (male, 4 weeks old) were s.c. inoculated with 3×10^6 SW1990 cells in the left abdomen. The tumors were allowed to grow for 6 d. The mice inoculated with tumor cells were randomly divided into three groups with 10 mice/group, including the control group, the low-dose ziprasidone group (100 mg/kg), and the high-dose ziprasidone group (200 mg/kg). Mice were given intragastric administration once a day. Tumor volume measurement and mouse body weight measurement were done as previously described [12].

3. Results

3.1 Identification of ziprasidone as a novel GOT1 inhibitor

Over 500 compounds were selected for preliminary activity assessment against GOT1 from the approved drug library [10]. Ziprasidone exhibited the best inhibitory activity on GOT1 with an IC_{50} value of 5.39 ± 1.13 μM (Fig. 1A). In order to explore the specificity of GOT1, malate dehydrogenase 1 (MDH1) was used as the control. The result indicated that the change of NADH content was related to the suppression of GOT1 enzyme activity, rather than MDH1. Ziprasidone exhibited potent GOT1 enzyme suppression activity and deserved more in-depth research.

3.2 Effects of ziprasidone on enzyme kinetics of GOT1

In order to explore the inhibitory mode of ziprasidone targeting GOT1, enzyme kinetics studies were applied to investigate the V_{max} and K_m of ziprasidone on GOT1. The results showed that ziprasidone had weak effect on the K_m of α-KG and reduced V_{max} dose-dependently, which is a typical non-competitive mode.

Table 1

GOT1 enzyme kinetic assay to evaluate the inhibition mode of ziprasidone.

Ziprasidone	α-KG			
(μM)	0	5	10	20
V_{max}(ΔRFU/min)	0.2197 ± 0.0087	0.1707 ± 0.0042	0.1371 ± 0.0075	0.1111 ± 0.0094
K_m(μM)	1.7180 ± 0.2679	1.6910 ± 0.1660	1.5810 ± 0.3532	1.6960 ± 0.5665

3.3 Ziprasidone specifically binds with GOT1 in vitro

The MST evaluation was further applied to explore the direct interaction between ziprasidone and GOT1, which showed the K_d value of 89.30 ± 5.35 μM (Fig. 1D). What's more, a DARTS experiment was carried out to detect the binding affinity between ziprasidone and GOT1. As shown in Fig. 1E-1F, ziprasidone enhanced GOT1 stability by binding to it without being degraded by pronase. These results indicated that ziprasidone could inhibit the activity of GOT1 by direct interaction.

3.4 Molecular docking shows the binding mode of ziprasidone and GOT1

To further clarify the binding conformation of ziprasidone with GOT1, molecular docking was performed [21]. The lowest-energy binding mode between ziprasidone and GOT1 was exhibited in Fig. 1G. Molecular docking results suggested that ziprasidone bound to an allosteric pocket of GOT1 (Fig. 1G). The binding domain of ziprasidone was located at the forefront of the catalytic active center, and some of the hydrophobic amino acid residues formed a hydrophobic pocket to hold ziprasidone, including Pro15, Val16, Phe19, Val38, and Tyr264 (Fig. 1H). The main hydrophobic interaction was formed between Arg42 and the carbonyl group of ziprasidone, and an apparent stacking was formed between Tyr264 and the indoline ring of ziprasidone. The predicted allosteric binding mode was consistent with the results that ziprasidone inhibited the enzyme activity of GOT1 in a non-competitive manner.

3.5 In vitro anti-proliferative activity of ziprasidone on SW1990 cells

Pancreatic cancer (SW1990), breast cancer (HCC1806), liver cancer (HepG2), colorectal cancer (HCT116, SW620, SW480), non-small cell lung cancer (A549), fibrosarcoma cells (HT1080), normal cells (L929) were initially selected to determine GOT1 expression level by western blotting. GOT1 is highly expressed in all tested cell lines except L929 (Fig. 2A). We attempted to evaluate whether ziprasidone could affect the cell viability of these cancer cells. The IC_{50} values of ziprasidone were measured in a variety of tumor cell lines and normal cell lines (Table 2). As shown in Fig. 2B, ziprasidone showed potent inhibitory activities on SW1990 cells growth.

Table 2

Inhibition of ziprasidone on all kinds of cell lines.

Cell	Ziprasidone (μM)
SW1990	27.19 ± 1.06
HT1080	14.04 ± 1.10
HepG2	>100
SW480	≈100
SW620	≈100
HCT116	>100
A549	>200
HCC1806	>50
MM-453	>100
MCF-7	35.86 ± 1.20
MM-231	>100
L929	>200
LO2	>200
Vero	>200
HPDE6C7	>100

3.6 Ziprasidone induces apoptosis in SW1990 cells

Based on the ability of ziprasidone inhibiting the viability of SW1990 cells, follow-up experiments were conducted to detect apoptosis-related indicators, including mitochondrial apoptosis pathway and death receptor apoptosis pathway. Ziprasidone could up-regulate the expression of cleaved caspase-3 and down-regulate the precursor of caspase-3 and caspase-9. Simultaneously inducing the cleavage of PARP,

a substrate of caspase-3, indicated that ziprasidone may stimulate cell death by activating caspase. The Bcl-2 family proteins in the mitochondrial apoptotic pathway were also tested and found that the expression of anti-apoptotic protein Bcl-2 was down-regulated, and pro-apoptotic protein Bax was up-regulated. It also proved that ziprasidone can promote the apoptosis of SW1990 cells (Fig. 2C, 2D). Hoechst 33342 staining was used to investigate the effect of ziprasidone on nuclear morphology. The SW1990 cells treated with ziprasidone showed significant chromatin condensation and fragmentation (Fig. 2E). Annexin-V/PI staining demonstrated that ziprasidone induced cell apoptosis in a dose-dependent manner (control: 0.27%, 20 μM: 10.94%, 40 μM: 70.07%) (Fig. 2F). In addition, ziprasidone induced cell cycle arrest at the G1 phase of SW1990 cells (Fig. 2G). The ability to form colonies of ziprasidone-treated SW1990 cells was down-regulated, indicating that ziprasidone can inhibit cell proliferation (Fig. 2H).

3.7 Ziprasidone suppresses *SW1990 cells proliferation and migration*

The results of the EdU proliferation experiment showed that the percentage of EdU^+ positive in SW1990 cells decreased after ziprasidone treatment, indicating that ziprasidone can inhibit the proliferation of SW1990 cells (Fig. 3A).

We performed the transwell experiment to investigate the inhibition of ziprasidone on the migration of SW1990 cells. As exhibited in Fig. 3B-3C, ziprasidone inhibited the migration of SW1990 cells in a dose-dependent manner. Furthermore, the scratch wound assay exhibited that ziprasidone evidently decreased the migration ability of SW1990 cells (Fig. 3D), which was consistent with the above results in transwell.

3.8 Ziprasidone modulates Gln metabolism and ROS response

Aspartic acid (Asp) and oxaloacetate (OAA) are the substrate and product of the GOT1 enzymatic reaction, respectively. Therefore, to a certain extent, OAA can rescue cells lacking glutamine metabolism, but Asp cannot [22]. In our experiment, SW1990 cells were pretreated with Asp and OAA, and then treated with ziprasidone to investigate whether OAA can antagonize ziprasidone. The results exhibited that the sensitivity of SW1990 cells on ziprasidone was significantly reduced when pretreated with OAA, while Asp pretreatment was basically unchanged (Fig. 3E). It proved that ziprasidone indeed inhibited the enzyme activity of GOT1 to further affect the production of cell metabolites. As a metabolite of glutamine, OAA maintains the redox homeostasis of PDAC by increasing the ratio of $NADPH/NADP^+$ [22]. Ziprasidone down-regulated the $NADPH/NADP^+$ ratio in a dose-dependent manner to destroy the redox state of SW1990 cells (Fig. 3F). Furthermore, ziprasidone induced ROS production in SW1990 cells dose-dependently (Fig. 3G). Therefore, we speculated that cells produced more reactive oxygen species (ROS) due to the inhibition of GOT1. These results indicated that the inhibition of ziprasidone can block the

production of Gln-dependent NADPH and participate in the redox state of PDAC cells (Fig. 3G). Furthermore, ziprasidone induced ROS production in SW1990 cells in a dose-dependent manner. After ziprasidone treatment, the extracellular acidification rate (ECAR) of SW1990 cells was significantly reduced, the same as respiration (oxygen consumption rate, OCR) (Fig. 3H, 3I). The above results indicate that ziprasidone inhibits malate-aspartate shuttle and mitochondrial respiration by inhibiting GOT1.

Ziprasidone activated the MAPKs signaling pathway by increasing the levels of p-Erk, p-p38, and p-JNK1/2. Ziprasidone inhibited autophagy in SW1990 cells by down-regulating the expression of LC3-ii (Fig. 4A, 4B).

We conducted an in-depth study on the ability of ziprasidone to inhibit GOT1. After knocking down the expression of GOT1, the inhibition of ziprasidone on the cell viability of SW1990 cells was significantly weakened (Fig. 4C, 4D). CETSA assay demonstrated that ziprasidone can significantly increase the thermal stability of GOT1 in the temperature range of 42-57°C (Fig. 4E). Both siRNA knockdown and CETSA prove that ziprasidone can directly target and bind with GOT1, and its biological function also depends on GOT1.

According to the previous results, it is known that the anti-tumor activity of ziprasidone involves multiple biological processes, including metabolism (BIP and G6PC3) [23, 24], oxidative stress (CHOP, GADD34 and HIF-1α) [25-27], cell cycle related (p21) [28] and autophagy (ATG5 and Beclin1) [29, 30]. Therefore, we tested the transcription level of key genes in the above process, and the results are consistent with the previous reports (Fig. 4F).

3.9 Ziprasidone treatment induces Gln metabolism and modulates mitochondria respiration

Metabolomics analysis of the metabolic regulation of ziprasidone on SW1990 was carried out by using UPLC-MS/MS. The fold change in metabolites content of ≥ 2 or ≤ 0.5 was defined as the differential metabolites. Compared with the control group, the expression of 119 metabolites was significantly different in the ziprasidone group. The quantitative data of up- or down-regulated metabolites were identified in Table S1, Fig. S1. After ziprasidone-treatment, the GOT1 enzyme-related metabolites changed significantly (Fig. 5B).

Furthermore, we performed cluster analysis of 119 differential metabolites through KEGG analysis to discover the biological significance of ziprasidone in regulating metabolism. 119 differential metabolites are mainly concentrated in glucose metabolism, nucleotide biosynthesis, amino acid biosynthesis and other pathways. What's more, ziprasidone could down-regulate the endogenous intermediate metabolites in the amino acid biosynthetic pathway of SW1990 cells (Fig. 5C, 5D). These results indicate that ziprasidone disrupts the metabolic process of SW1990 cells by targeting inhibition of GOT1.

3.10 Ziprasidone suppresses tumor growth in SW1990 xenograft model

GOT1 is commonly expressed in malignant pancreatic cancers. Based on the results of ziprasidone inhibiting the growth of SW1990 cells, we constructed a xenograft tumor model of SW1990 cells to investigate the *in vivo* inhibitory activity of ziprasidone. Three groups of SW1990 xenograft CB-17/Icr-scid mice were intragastric administrated with ziprasidone (200, 100 mg/kg) or vehicle once a day. The tumor volume of mice decreased significantly after two weeks of treatment with ziprasidone compared with the control group. The tumor weights of the 100 mg/kg and 200 mg/kg ziprasidone treatment groups decreased by 75.29% and 84.54%, respectively (Fig. 6B, 6D). As shown in Fig. 6A, after treated with 200 mg/kg ziprasidone, a decrease in mice body weight, and lethargy and anorexia were observed. H&E staining of the spleen, kidney and pancreas of mice showed no difference between the treated group and control group, indicating that ziprasidone did not damage the internal organs of mice (Fig. S2).

In order to further investigate the effect of ziprasidone on the metastasis and growth of solid tumors, H&E staining was performed on liver tissues and immunohistochemical analysis was performed on tumor tissues. H&E staining results showed that ziprasidone inhibited tumor cell metastasis to the liver. In addition, the tumor marker CD133 immunohistochemical results showed that ziprasidone can inhibit tumor growth (Fig. 6E).

Discussion

Glutamine-mediated metabolic reprogramming can not only maintain redox homeostasis, but also provide raw materials for biosynthesis and TCA cycle of PDAC cells proliferation. Targeting inhibition of GOT1 to disrupt tumor metabolic homeostasis, which is an important strategy for us to find promising anti-tumor drug candidates. At present, the development of GOT1 inhibitors is still in the preliminary exploration stage. We hope that our long-term research can provide a strategy for the treatment of tumors that rely on glutamine metabolism.

Compared with the development of a brand-new drug for a certain indication, drug repurposing has obvious advantages, including reducing the risk and investment, and shortening the drug research and development time. Our research group is committed to the development of GOT1 inhibitors, and previous work has found lead compounds with good activity in natural products [12]. However, for PDAC, a fatal malignant tumor, no effective treatment has been found so far. There is an urgent need to develop drug candidates for treating PDAC. Based on the significance of GOT1 for PDAC to maintain redox homeostasis and the urgency of drug candidate discovery, we tried to find potential drug candidates through the strategy of drug repurposing.

The antipsychotic drug ziprasidone displayed significant *in vitro* and *in vivo* antitumor efficacy by inhibiting GOT1. High-dose 200 mg/kg ziprasidone was administered to SW1990 cell xenograft tumor model, and no obvious adverse reactions were found. Regarding the safety of ziprasidone, Pfizer-Spain

has recorded four cases of ziprasidone overdose, the highest of which was 4480 mg. QTc interval is within the normal range in all patients and there are no cardiac side effects, which suggests that overdose of ziprasidone may be relatively safe in patients without risk factors that contraindicate its use [31]. In this study, although our dosage of ziprasidone (100 mg/kg and 200 mg/kg) may be higher than its clinical dose (maximum recommended dose as 80 mg twice a day in particular cases), these doses are lower than the toxic dose suggested in the literature. Although, we observed a decrease in mice body weight in 200 mg/kg ziprasidone treated group, no apparent organ damage in spleen, kidney and pancreas were observed. Because we also observed lethargy and anorexia in this group of animals, we speculated that the major reason for the loss of body weight might be the reduced uptake of foods. Although there was a little weight loss in the high-dose group, the anti-tumor effect of ziprasidone was not influenced.

Conclusions

The enzyme activity inhibition experiment showed that ziprasidone had obvious inhibition effect on GOT1, and the inhibitory effects on related tumor cells were proved by the related pharmacological experimental evaluation. The new indications of ziprasidone provide a new approach for the treatment of tumors. These findings may have implications for future treatments of PDAC (Fig. 7).

Abbreviations

PDAC: Pancreatic ductal adenocarcinoma; GOT1: glutamate-oxaloacetate transaminase 1; 2-DG: 2-Deoxyglucose; FCCP: Carbonyl cyanide 4-(trifluoromethoxy)phenylhydrazone; ECAR: Extracellular Acidification Rate; OCR: Oxygen Consumption Rate; TCA: tricarboxylic acid; NEAA: non-essential amino acids; GLUD1: glutamate dehydrogenase 1; OAA: oxaloacetic acid; AOA: Aminooxyacetate; 5-HT2: serotonin Type 2; D2: dopamine Type 2; MST: Microscale thermophoresis; CETSA: cellular thermal shift assay; PVDF: Polyvinylidene difluoride membranes; H&E: Hematoxylin-eosin; PARP: poly-(ADP-ribose) polymerase; IHC; immunohistochemistry Chemical compound studied in this article

Declarations

Author contributions

Yueying Yang, Fei Han and Mingxue Li: acquisition of data, analysis and interpretation of data, statistical analysis and drafting of the manuscript; Mengzhu Zheng and Xiaoxia Gu carried out parts of the experiments; Hua Li and Lixia Chen study concept and design, analysis and interpretation of data, critical revision of the manuscript for important intellectual content, obtained study funding, and study supervision. All authors have read and approved the manuscript for publication.

Funding

We acknowledge support from National Natural Science Foundation of China (NSFC) (grant number 81773594, 81903863, 31270399, U1803122, 81773637), National Mega-project for Innovative Drugs (grant number 2019ZX09721001-004-007), the Fundamental Research Fund for the Central Universities (grant number 2017KFYXJJ151), China Postdoctoral Science Foundation (grant number 2019M652661), Chunhui Program-Cooperative Research Project of the Ministry of Education, Liaoning Revitalization Talents Program (No. XLYC1807182), and Liaoning Province Natural Science Foundation (No. 2020-MZLH-31, 2019-MS-299).

Data availability statement

The data will be made available upon reasonable request.

Ethics approval and consent to participate

All procedures in this study were performed in accordance with the ethical standards of the Animal Care and Use Committee of Shenyang Pharmaceutical University.

Declaration of competing interest

The authors declare that they have no competing interests.

Ziprasidone (PubChem CID: 60854)

References

1. Luengo A, Gui DY, Vander HM. Targeting metabolism for cancer therapy. Cell Chem Biol 2017;24(9):1161-1180.
2. Rahib L, Smith BD, Aizenberg R, Rosenzweig AB, Fleshman JM, Matrisian LM. Projecting cancer incidence and deaths to 2030: the unexpected burden of thyroid, liver, and pancreas cancers in the United States. Cancer Res 2014;74(11):2913-2921.
3. Camelo F, Le A. The intricate metabolism of pancreatic cancers. Adv Exp Med Biol 2018;1063:73-1081.
4. Son J, Lyssiotis CA, Ying H, Wang X, Hua S, Ligorio M, Perera RM, Ferrone CR, Mullarky E, Shyh-Chang N, Kang Y, Fleming JB, Bardeesy N, Asara JM, Haigis MC, DePinho RA, Cantley LC, Kimmelman AC. Glutamine supports pancreatic cancer growth through a KRAS-regulated metabolic pathway. Nature 2013;496(7443):101-105.
5. Chae YC, Kim JH. Cancer stem cell metabolism: target for cancer therapy. BMB Rep 2018;51(7):319-326.

6. DeBerardinis RJ, Cheng T. Q's next: the diverse functions of glutamine in metabolism, cell biology and cancer. Oncogene 2010;29(3):313-324.
7. Shanware NP, Mullen AR, DeBerardinis RJ, Abraham RT. Glutamine: pleiotropic roles in tumor growth and stress resistance. J Mol Med (Berl) 2011;89(3):229-236.
8. Cluntun AA, Lukey MJ, Cerione RA, Locasale JW. Glutamine metabolism in cancer: understanding the heterogeneity. Trends Cancer 2017;3(3):169-180.
9. Zhou X, Curbo S, Li F, Krishnan S, Karlsson A. Inhibition of glutamate oxaloacetate transaminase 1 in cancer cell lines results in altered metabolism with increased dependency of glucose. Bmc Cancer 2018;18(1):559.
10. Anglin J, Zavareh RB, Sander PN, Haldar D, Mullarky E, Cantley LC, Kimmelman AC, Lyssiotis CA, Lairson LL. Discovery and optimization of aspartate aminotransferase 1 inhibitors to target redox balance in pancreatic ductal adenocarcinoma. Bioorg Med Chem Lett 2018;28(16):2675-2678.
11. Holt MC, Assar Z, Beheshti ZR, Lin L, Anglin J, Mashadova O, Haldar D, Mullarky E, Kremer DM, Cantley LC, Kimmelman AC, Stein AJ, Lairson LL, Lyssiotis CA. Biochemical characterization and structure-based mutational analysis provide insight into the binding and mechanism of action of novel aspartate aminotransferase inhibitors. Biochemistry 2018;57(47):6604-6614.
12. Sun W, Luan S, Qi C, Tong Q, Yan S, Li H, Zhang Y. Aspulvinone O, a natural inhibitor of GOT1 suppresses pancreatic ductal adenocarcinoma cells growth by interfering glutamine metabolism. Cell Commun Signal 2019;17(1):111.
13. Duarte T, Barbisan F, Do PP, Azzolin VF, da Cruz Jung IE, Duarte MMMF, Teixeira CF, Mastella MH, da Cruz IBM. Ziprasidone, a second-generation antipsychotic drug, triggers a macrophage inflammatory response *in vitro*. Cytokine 2018;106:101-107.
14. Jiang X, Chang H, Zhou Y. Expression, purification and preliminary crystallographic studies of human glutamate oxaloacetate transaminase 1 (GOT1). Protein Expr Purif 2015;113:102-106.
15. Wang Q, Zhang Q, Luan S, Yang K, Zheng M, Li K, Chen L, Li H. Adapalene inhibits ovarian cancer ES-2 cells growth by targeting glutamic-oxaloacetic transaminase 1. Bioorg Chem 2019;93:103315.
16. Min Q, Cai X, Sun W, Gao F, Li Z, Zhang Q, Wan LS, Li H, Chen J. Identification of mangiferin as a potential glucokinase activator by structure-based virtual ligand screening. Sci Rep 2017;7:44681.
17. Zheng M, Wu C, Yang K, Yang Y, Liu Y, Gao S, Wang Q, Li C, Chen L, Li H. Novel selective hexokinase 2 inhibitor Benitrobenrazide blocks cancer cells growth by targeting glycolysis. Pharmacol Res. 2021;164:105367.
18. Gao Y, Zhu L, Guo J, Yuan T, Wang L, Li H, Chen L. Farnesyl phenolic enantiomers as natural MTH1 inhibitors from Ganoderma sinense. Oncotarget 2017;8(56):95865-95879.
19. Martinez MD, Jafari R, Ignatushchenko M, Seki T, Larsson EA, Dan C, Sreekumar L, Cao Y, Nordlund P. Monitoring drug target engagement in cells and tissues using the cellular thermal shift assay. Science 2013;341(6141):84-87.
20. Alshareef A, Zhang HF, Huang YH, Wu C, Zhang JD, Wang P, El-Sehemy A, Fares M, Lai R. The use of cellular thermal shift assay (CETSA) to study crizotinib resistance in ALK-expressing human cancers.

Sci Rep 2016;6:33710.
21. Abagyan MTDK R. ICM-A new method for protein modeling and design: applications to docking and structure prediction from the distorted native conformation. J Comput Chem 1994;5(15):488-506.
22. Wang YP, Zhou W, Wang J, Huang X, Zuo Y, Wang TS, Gao X, Xu YY, Zou SW, Liu YB, Cheng JK, Lei QY. Arginine methylation of MDH1 by CARM1 inhibits glutamine metabolism and suppresses pancreatic cancer. Mol Cell 2016;64(4):673-687.
23. Girona J, Rodríguez-Borjabad C, Ibarretxe D, Vallvé J-C, Ferré R, Heras M, Rodríguez-Calvo R, Guaita-Esteruelas S, Martínez-Micaelo N, Plana N, Masana L. The Circulating GRP78/BiP Is a Marker of Metabolic Diseases and Atherosclerosis: Bringing Endoplasmic Reticulum Stress into the Clinical Scenario. J Clin Med. 2019;8(11):1793.
24. Dienel GA. Hypothesis: A Novel Neuroprotective Role for Glucose-6-phosphatase (G6PC3) in Brain-To Maintain Energy-Dependent Functions Including Cognitive Processes. Neurochem Res. 2020;45(11):2529-2552.
25. Ariyama Y, Tanaka Y, Shimizu H, Shimomura K, Okada S, Saito T, Yamada E, Oyadomari S, Mori M, Mori M. The role of CHOP messenger RNA expression in the link between oxidative stress and apoptosis. Metabolism. 2008;57(12):1625-1635.
26. Lee IC, Ho XY, George SE, Goh CW, Sundaram JR, Pang KKL, Luo W, Yusoff P, Sze KSW, Shenolikar S. Oxidative stress promotes SIRT1 recruitment to the GADD34/PP1α complex to activate its deacetylase function. Cell Death Differ. 2018;25(2):255-267.
27. Li HS, Zhou YN, Li L, Li SF, Long D, Chen XL, Zhang JB, Feng L, Li YP. HIF-1α protects against oxidative stress by directly targeting mitochondria. Redox Biol. 2019;25:101109.
28. El-Deiry WS. p21(WAF1) Mediates Cell-Cycle Inhibition, Relevant to Cancer Suppression and Therapy. Cancer Res. 2016;76(18):5189-5191.
29. Galluzzi L, Green DR. Autophagy-Independent Functions of the Autophagy Machinery. Cell. 2019;177(7):1682-1699.
30. Kang R, Zeh HJ, Lotze MT, Tang D. The Beclin 1 network regulates autophagy and apoptosis. Cell Death Differ. 2011;18(4):571-580.
31. Gomez-Criado MS, Bernardo M, Florez T, Gutiérrez JR, Gandía R, Ayani I. Ziprasidone overdose: cases recorded in the database of Pfizer-Spain and literature review. Pharmacotherapy 2005;25(11):1660-1665.

Figures

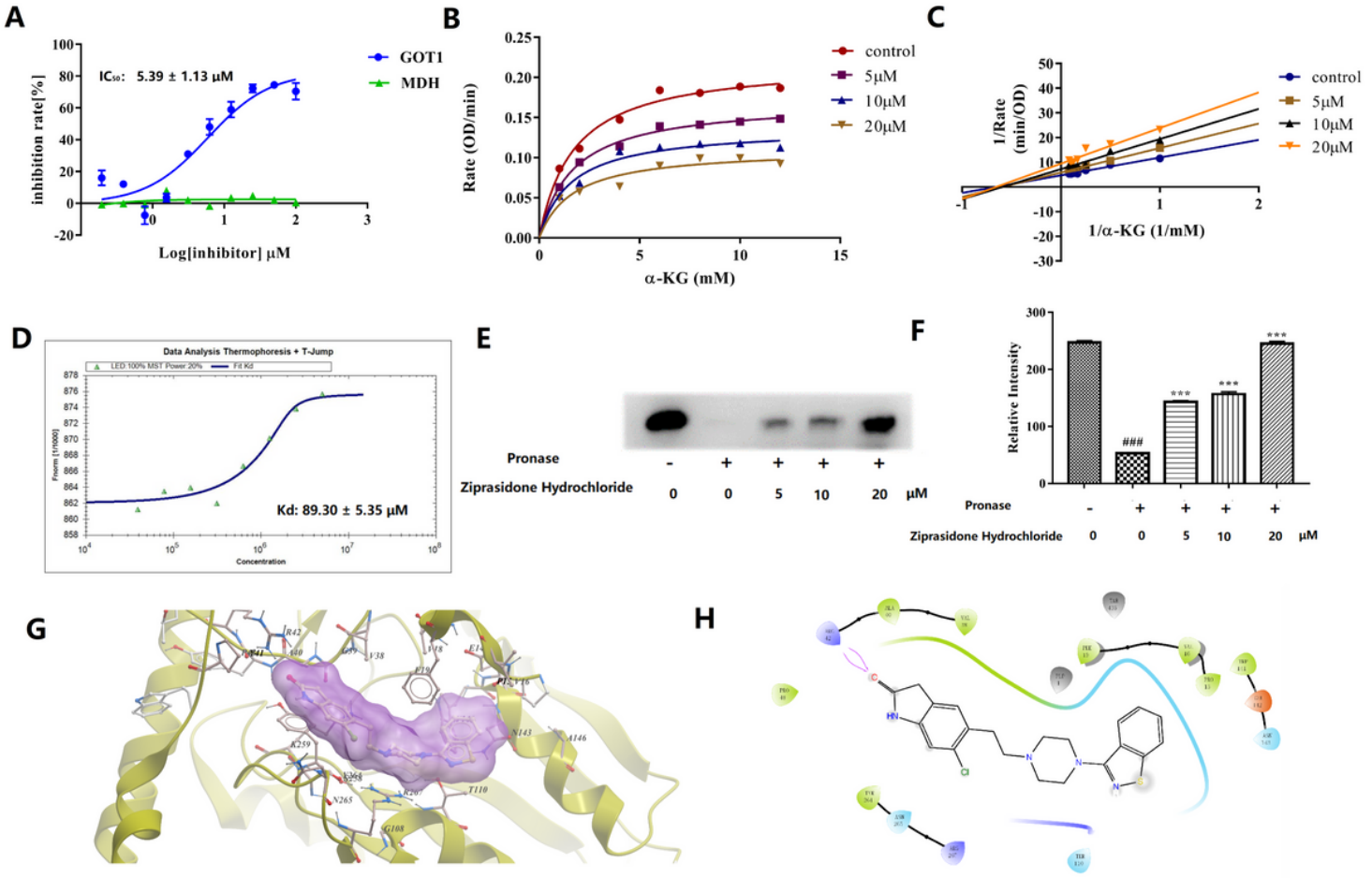

Figure 1

Enzyme kinetics research and the binding ability evaluation between ziprasidone and GOT1. (A) The selective inhibition of ziprasidone on GOT1 and MDH. (B) The α-KG saturation curves of ziprasidone on GOT1 at different concentrations (5 μM-20 μM). (C) The α-KG saturation curves for GOT1 with different concentrations of ziprasidone via double-reciprocal plot Line weaver-Burk. (D) Binding affinity between ziprasidone and GOT1 by MST assay. (E, F) DARTS experiment to investigate the ability of ziprasidone to stabilize GOT1 by preventing from being hydrolyzed. Data are mean ± SD, (n = 5). (G) Detailed view of ziprasidone and the allosteric activity center amino acid residues of GOT1. (H) Ligand interaction mode of ziprasidone with GOT1.

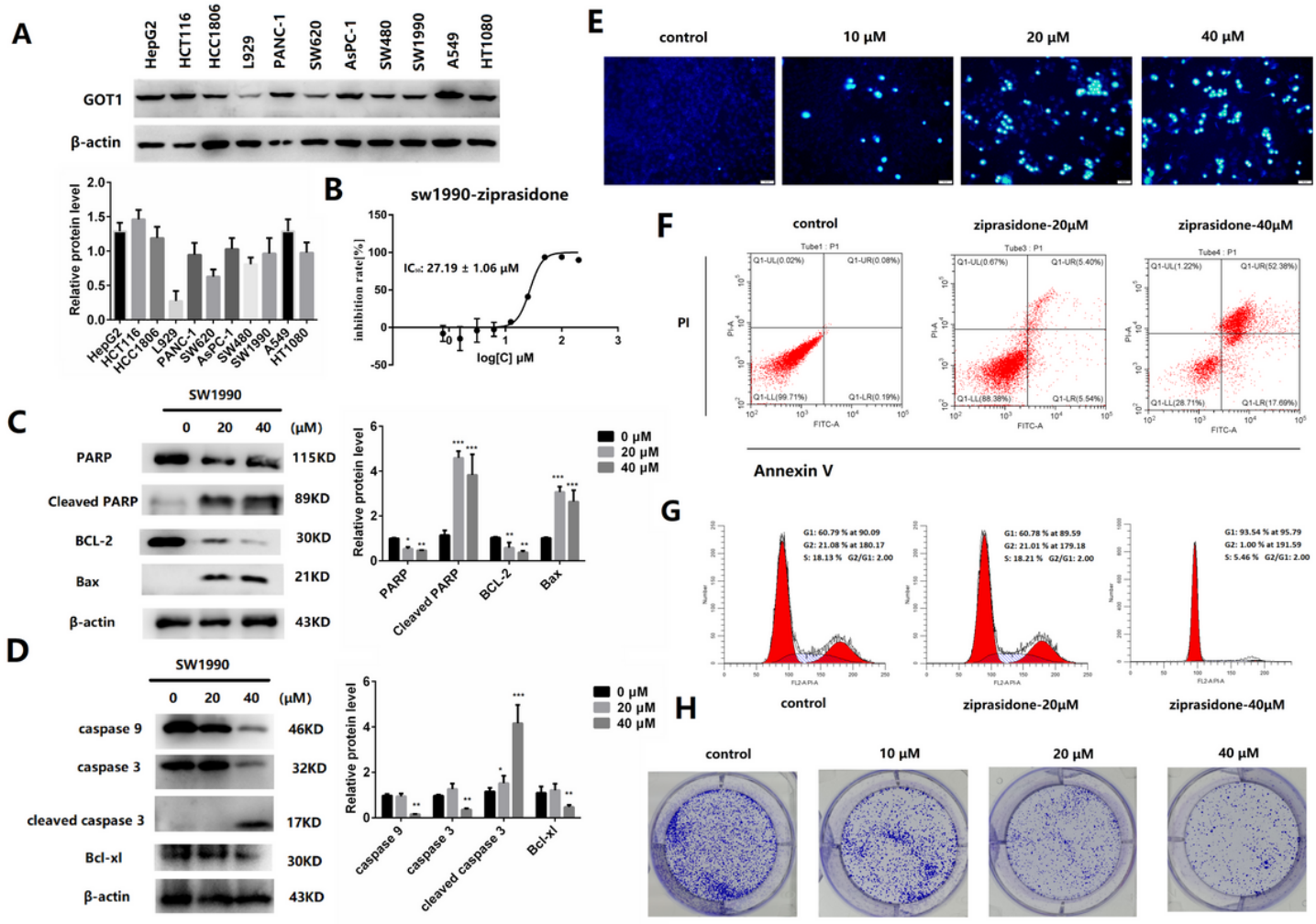

Figure 2

The evaluation of ziprasidone on anti-proliferative activity in vitro. (A) Up: Expression of GOT1 was evaluated by Western blot in SW1990, PANC-1, AsPC-1, HCC1806, HepG2, HCT116, SW620, SW480, A549, HT1080 and L929. (B) The effects of anti-proliferative activity of ziprasidone on SW1990 cells via MTT assays. (C, D) Detection of apoptosis-related protein expression in SW1990 cells treated with different concentrations of ziprasidone by Western blot. Data are mean SD, (n = 5). *p value < 0.05 compared with control group. (E) Hoechst 33342 staining to observe the chromatin changes of SW1990 cells after ziprasidone treatment. (F) Annexin V/PI staining to analyze the apoptosis effect of ziprasidone on SW1990 cells. (G) Flow cytometry analysis of the effect of ziprasidone on the cell cycle of SW1990. (H) Clone formation experiment to evaluate the effect of ziprasidone on the proliferation of SW1990 cells.

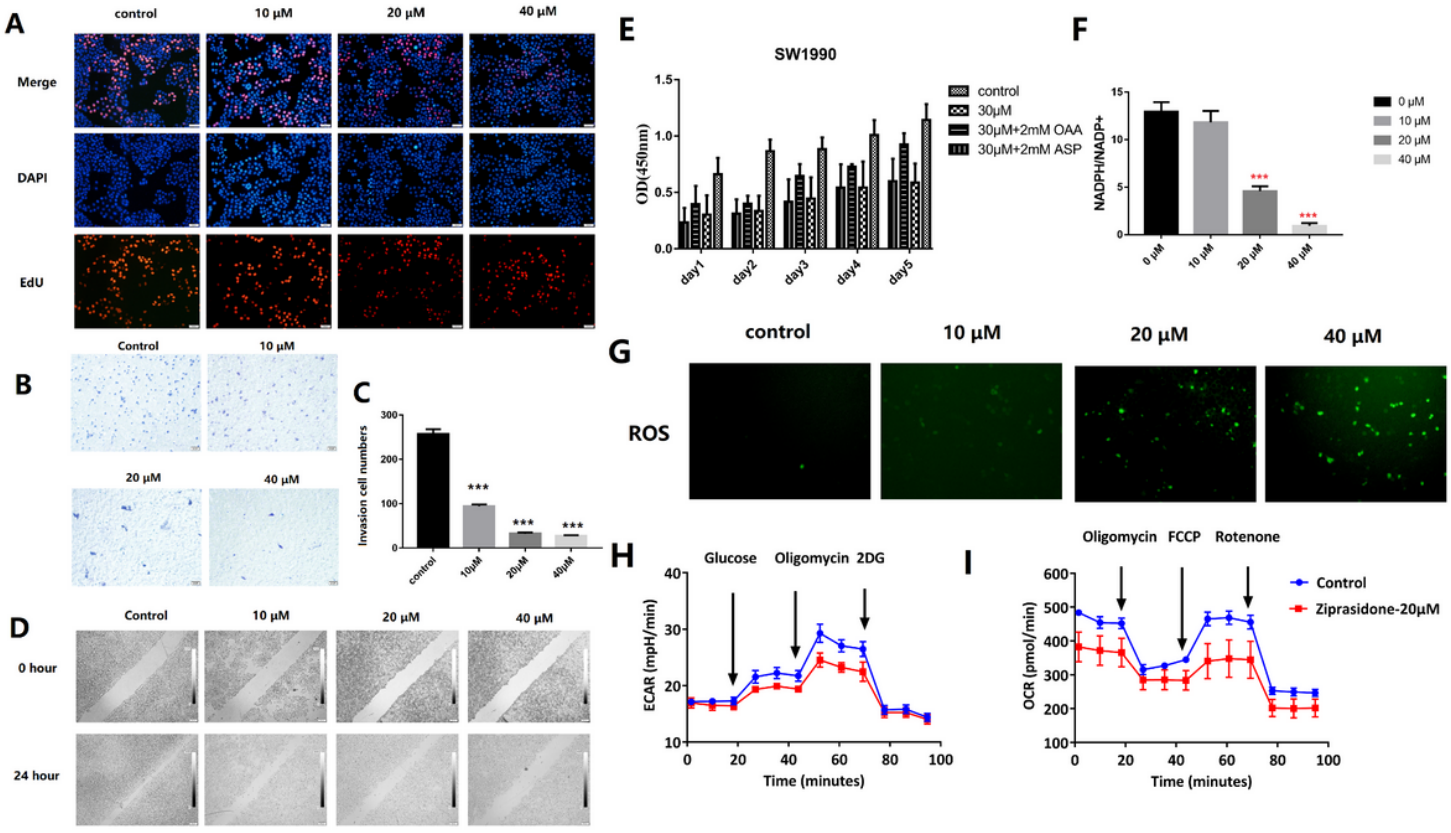

Figure 3

Ziprasidone inhibited SW1990 cells proliferation and migration in a dose-dependent manner and ziprasidone treatment induced Gln metabolism and modulated mitochondria respiration. (A) The proportion of cell proliferation was evaluated by EdU. (B, C) Transwell assay and quantitative analysis. (D) A phase contrast microscope was used to take pictures of wound healing from scratches at 0 h and 24 h after the scratch. (E) SW1990 cells were pretreated with OAA, ASP, respectively, and then treated with ziprasidone, the number of cells was determined. (F) To evaluate the NADP+/NADPH ratio of SW1990 cells after treatment with different concentrations of ziprasidone. (G) Intracellular ROS in control and ziprasidone treatment were measured. (H, I) OCR and ECAR analyses to evaluate the effects of ziprasidone on redox status of SW1990 cells. Data are mean SD, (n = 5). *p value < 0.05 compared with cells control group.

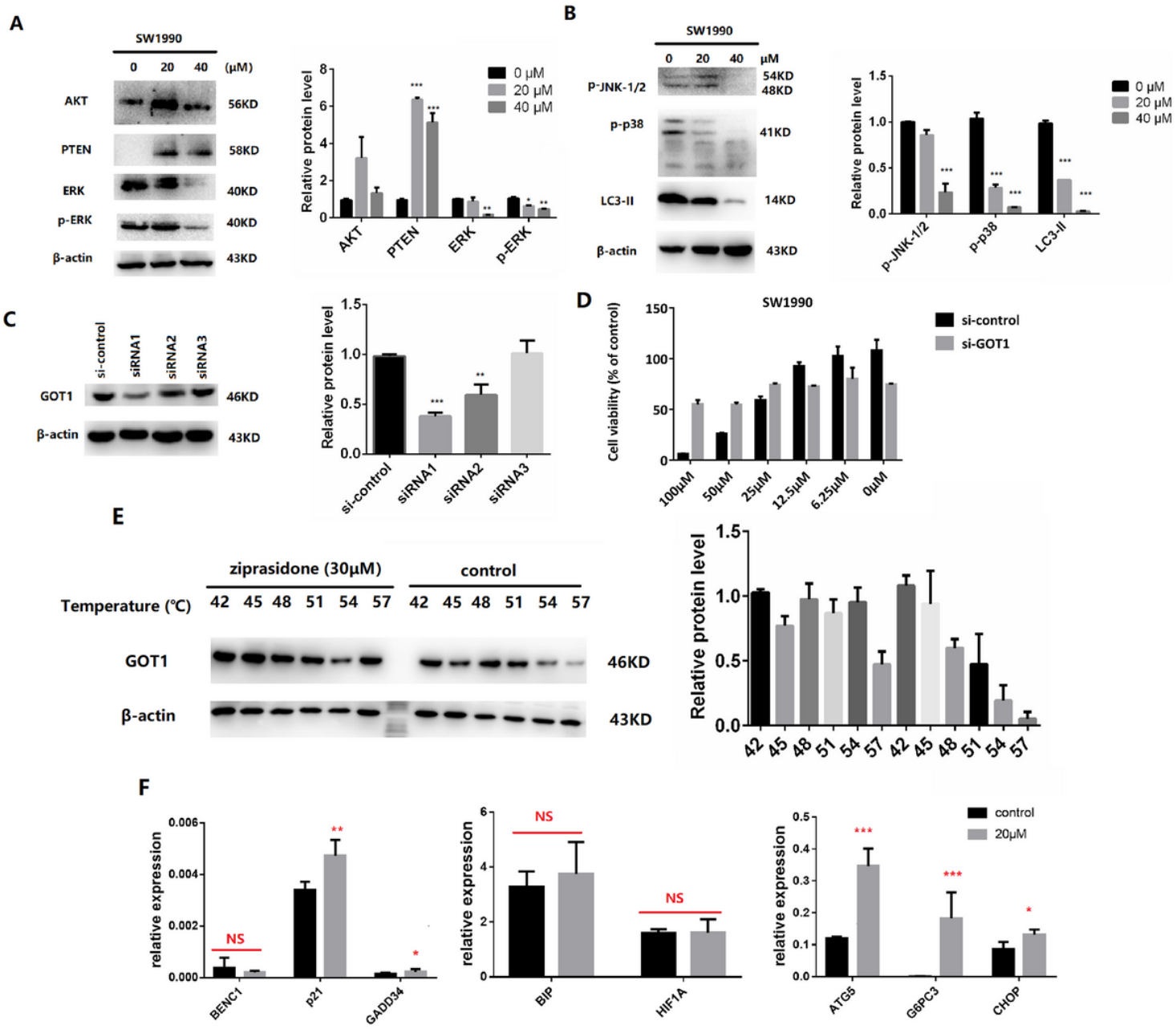

Figure 4

Ziprasidone targeted GOT1 to induce SW1990 cells apoptosis. (A, B) Western blot in SW1990 cells. Analysis of Western blot results in (A, B). (C) Knockdown efficiency of GOT1 expression after transfection of siRNA in SW1990 cells by Western blot analysis. (D) The cytotoxicity of ziprasidone on the PDAC cells was remarkably decreased. (E) A cellular thermal shift assay to evaluate the binding ability of ziprasidone with GOT1. (F) The transcription of metabolism, oxidative stress and growth arrest related genes after treatment with ziprasidone on SW1990 cells. Data are mean ± SD, (n = 5). *p value < 0.05, **p value < 0.01, ***p value < 0.001 compared with cells control group.

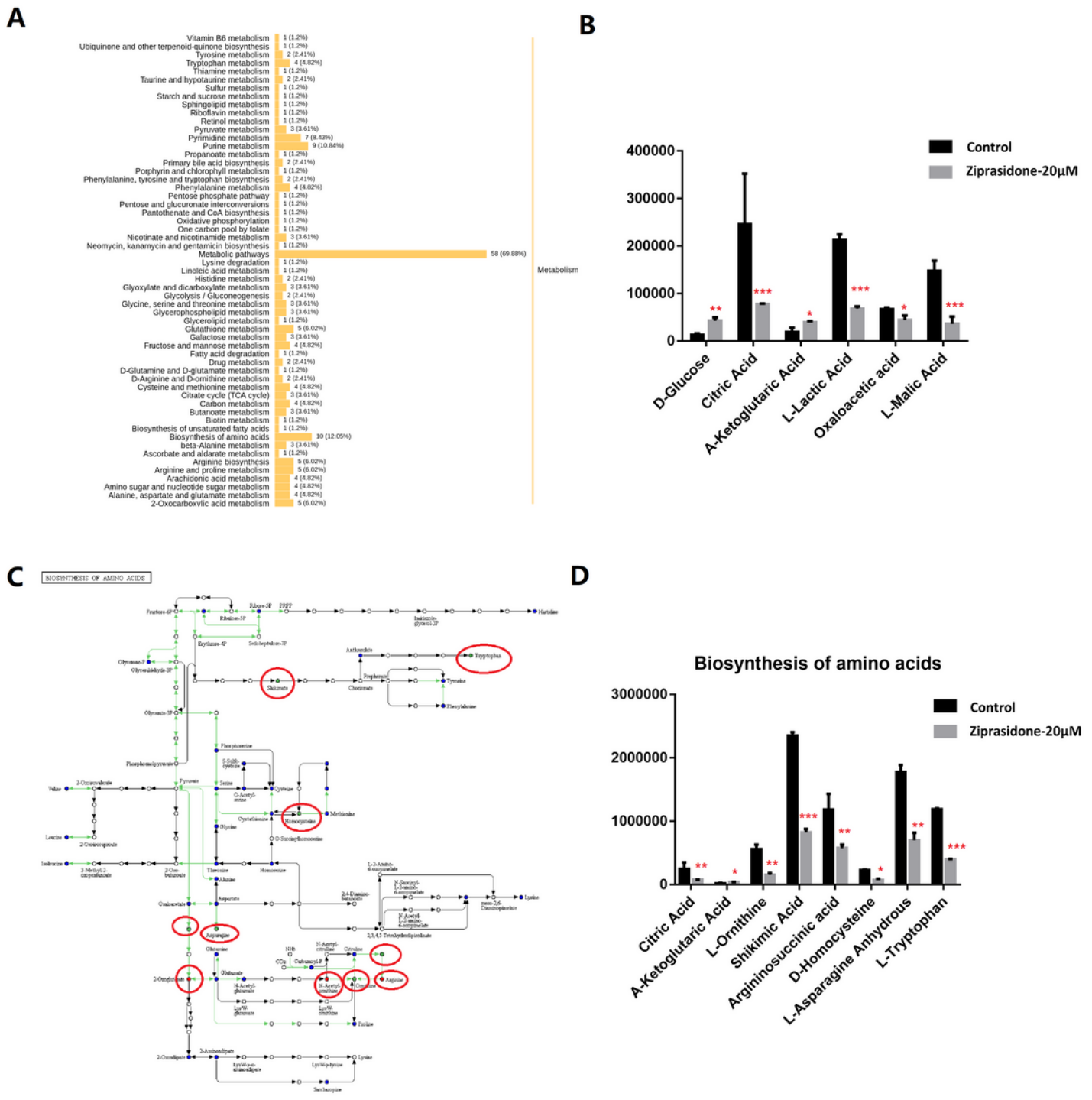

Figure 5

Ziprosidone suppresses cancer cell metabolism. (A) Classification of metabolites in SW1990 cells after treated by ziprasidone. The ordinate represents metabolic pathways. The abscissa represents the number and proportion of metabolites involving in the metabolic pathway. (B) The change of GOT1 enzyme-related metabolites after ziprasidone treatment. (C, D) Changes of intermediate metabolites in the amino acid biosynthetic pathway after SW1990 cells treatment with ziprasidone. Red, blue and green respectively represent the up-regulation, no significant change or down-regulation of metabolite content

after ziprasidone treatment. Data are mean ± SD, (n = 5). * p <0.05, ** p < 0.01, *** p < 0.001 compared with the control by t-test.

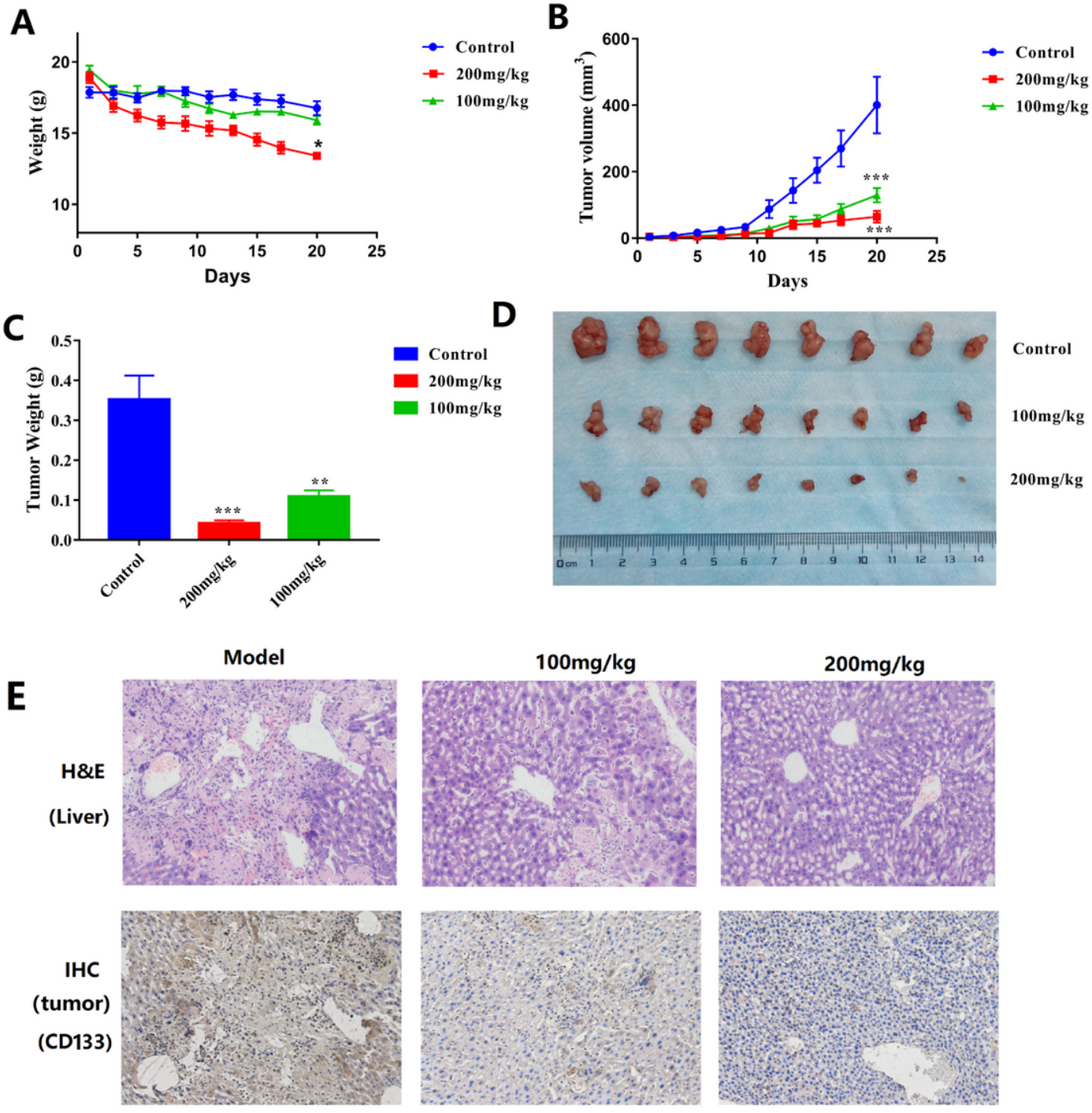

Figure 6

In vivo study of the inhibitory effect of ziprasidone on SW1990 cell xenograft tumor model. (A) Record the weight of mice in the control group (n = 10), low-dose ziprasidone group (100 mg/kg, n=10) and high-dose ziprasidone group (200 mg/kg, n = 10) within 20 days. (B) Record the tumor volume of mice in the control group (n = 10), low-dose ziprasidone group (100 mg/kg, n = 10) and high-dose ziprasidone group

(200 mg/kg, n = 10) within 20 days. (C) Average tumor weight of the three groups after 20 days of ziprasidone administration. (D) The solid tumor image of control group, low-dose ziprasidone group and high-dose ziprasidone group. (E) H&E staining of mouse liver tissue to evaluate the inhibition of ziprasidone on tumor metastasis. The inhibition of ziprasidone on the expression of tumor hepatocyte marker CD133 was evaluated by immunohistochemistry. Data are mean ± SD, (n = 10). * p <0.05, ** p < 0.01, *** p < 0.001 compared with the control by t-test.

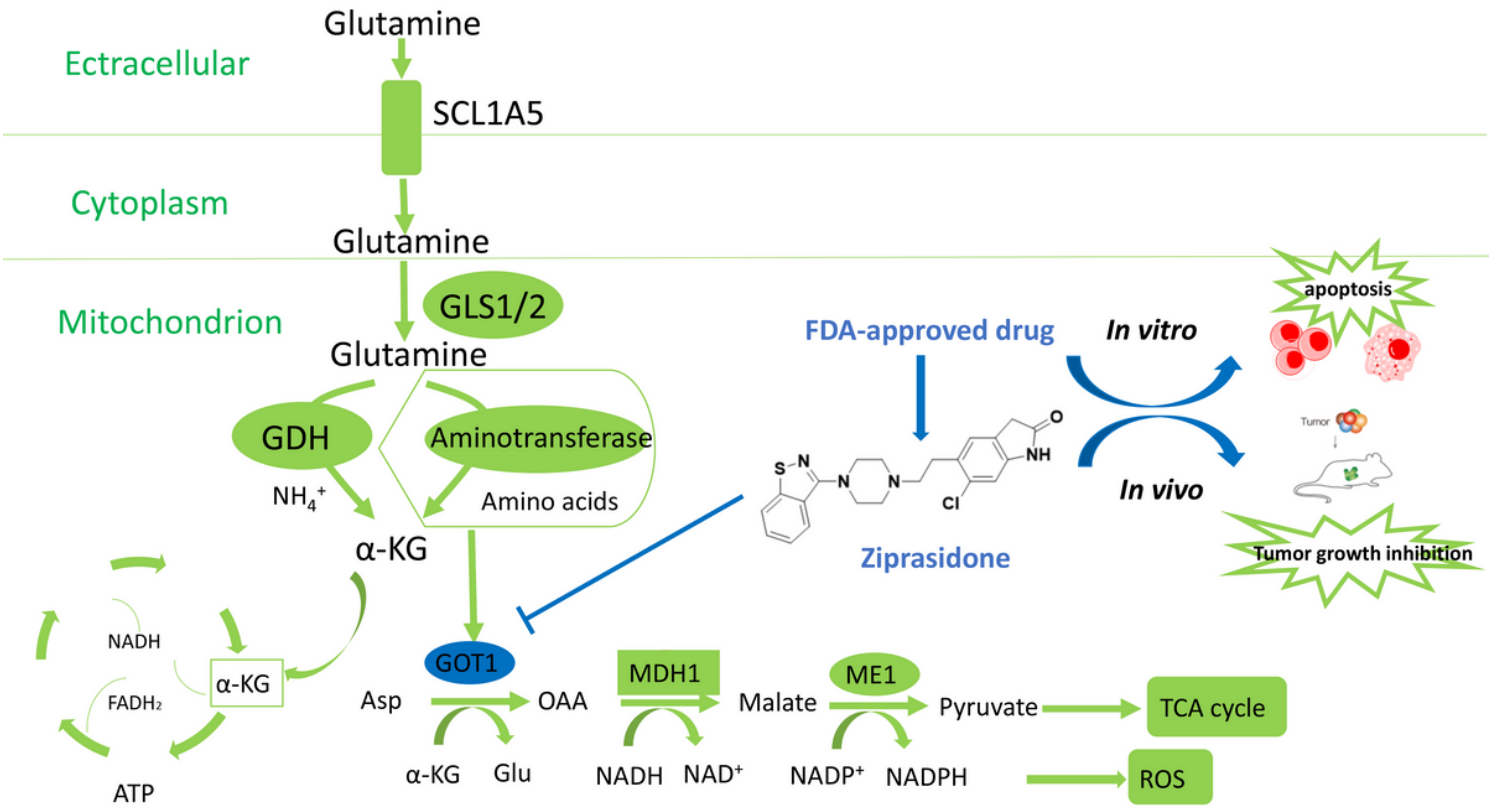

Figure 7

The potential cytotoxicity and anti-proliferation effects of a novel GOT1 inhibitor (ziprasidone) against pancreatic adenocarcinoma cells in vitro and in vivo were summarized.

Supplementary Files

This is a list of supplementary files associated with this preprint. Click to download.

- GraphicalAbstract.tif
- FigureS1.tif
- FigureS2.tif
- Supplementary.TableS.xlsx